8-2017

Effects of Acute Sepsis on Renal Structure and Sympathetic Innervation in Mice

Tuqa Alkhateeb
East Tennessee State University

Follow this and additional works at: https://dc.etsu.edu/etd

Part of the Animals Commons, Biology Commons, Infectious Disease Commons, Nephrology Commons, and the Pathology Commons

Effects of Acute Sepsis on Renal Structure and Sympathetic Innervation in Mice

_____

A thesis

presented to

the faculty of the Department of Biological Sciences

East Tennessee State University

In partial fulfillment

of the requirements for the degree

Master of Science in Biology

_____

by

Tuqa Alkhateeb

August 2017

_____

Donald B. Hoover, PhD, Chair

Thomas C. Jones, PhD

Tammy R. Ozment, DVM, PhD

Keywords: acute sepsis, sympathetic innervation, renal structure, non-neuronal cholinergic cells, kidney function, tyrosine hydroxylase, catecholamines.

ABSTRACT

Effects of Acute Sepsis on Renal Structure and Sympathetic Innervation in Mice

by

Tuqa Alkhateeb

Sympathetic nerves are important for renal physiology and sepsis pathophysiology. A recent study showed sprouting of sympathetic nerves in spleen of septic mice. This study was done to test if renal sprouting of sympathetic nerves also happens and to investigate renal morphology in septic mice. Cecal ligation and puncture (CLP) was used to induce sepsis and kidneys were removed for evaluation. Bowman's space was diminished with cortical bubble cells present suggestive of acute renal pathology, however, renal function was unchanged. Acute sepsis did not affect either renal sympathetic innervation or non-neuronal cholinergic cells. Mouse kidneys had more epinephrine (EPI) than norepinephrine (NE) in both groups. This is most likely due to uptake of epinephrine by renal sympathetic nerves and may have no correlation with sepsis. In conclusion, septic mice showed minor renal pathology and no evidence of acute sympathetic nerve sprouting. Further studies are needed to understand the mechanism and consequences of elevated EPI in mice kidney.

DEDICATION

I dedicate this work to my unconditionally loving and caring parents, my father Dr. Faisal Alkhateeb and my mother Faten Jaradat. Their wisdom, support and encouragement have been the main reason of who I am today and what I have achieved thus far. I will never be able to thank them enough. This work is also dedicated to my wonderful siblings that were with me through all the thick and thin, Thabit, Hassan, Hiba and Kenan.

ACKNOWLEDGEMENTS

TABLE OF CONTENTS

LIST OF FIGURES

CHAPTER 1

INTRODUCTION

Sepsis

Each year in the US, around 600,000 patients are diagnosed with the deadly spectrum of sepsis, with a mortality rate of 28-50% (Rangel-Frausto et al. 1995; Zeni et al. 1997; Angus et al. 2001; Martin et al. 2003). Moreover, the cost per year of care given for septic patients is estimated to be $24 billion (Torio and Moore 2013). From 2004 until 2009, severe sepsis showed an average annual increase of 13% with the cumulative number of patients dying from sepsis rising over the years (Zarjou and Agarwal 2011). Sepsis usually starts off with an infection such as pneumonia, an intra-abdominal, urinary or skin/wound infection that may later develop into sepsis if not treated properly. Gram positive/negative bacteria are usually the source of infection in septic patients although fungal or protozoal agents may also be a cause (Pavlidis 2003; Kalra and Raizada 2006; Gaieski et al. 2010; Martin 2012). Moreover, the diagnosis of septic patients is not always direct as its symptoms are very similar to other diseases (Cunha and Shea 1996).

Sepsis is identified as a confirmed infection along with at least two signs of the systemic inflammatory response syndrome (SIRS) (Martin 2012). SIRS is a massive state of inflammation throughout the body that may involve the patient having abnormal body temperature ($<36°C$ or $>38°C$), respiration rate greater than 20/min, a heart rate greater than 90/min and white blood count to be greater than $12,000/mm^3$ or less than $4000/mm^3$ (Annane et al. 2005). If sepsis is not treated, then severe sepsis might develop that includes the septic symptoms along with organ dysfunction (Levy et al. 2003).

Early recognition and treatment may be life-saving; therefore if appropriate therapy is given within 6 h of suspected diagnosis, the patient's chance of survival is improved (Iskander et al. 2013). However, even after receiving treatment, the patient is still at a high risk for repeated infections and organ damage with a diminished quality of life (Gentile et al. 2012). The human host system might differ between individuals when reacting to the early overwhelming inflammation stage due to many issues such as patient's age, genetic factors, comorbidities, immunocompetence, as well as the virulence of the microbes (Boomer et al. 2014), and therefore, an individualized therapy is required. Certain guidelines and protocols are helpful to direct treatment in improving septic patients' survival. The recommendations include early disease recognition, rapid aggressive IV fluid resuscitation with 0.9% normal saline for tissue reperfusion, oxygen support, broad-spectrum antibiotics given as empiric therapy (Howell and Davis 2017) and sometimes use of vasopressors in septic shock (Beale et al. 2004). Moreover, the source of infection can be eradicated by removing the infected or necrotic tissue and drainage of pus.

Pathophysiology of Initial Inflammatory Stage

Sepsis is characterized as a SIRS in response to an infection, stimulated by production of initial proinflammatory cytokines such as IL-1, TNF-α, IL- 12, IL-8, IL-6, high mobility group box 1 (HMGB1) and acute phase proteins (Charalambos et al. 2000; Chaudhry et al. 2013; Xiao et al. 2015). Currently, there are still not enough details describing the exact pathways underlying the pathophysiology of sepsis to help prevent the development of SIRS and sepsis in humans. In the primary stage of sepsis, a 'cytokine storm' is thought to occur with intense interaction between the infectious organisms and the host pathogen-recognition system or innate immunity (Boomer et al. 2011; Chaudhry et al. 2013). The interaction is characterized by

9

pathogen-associated molecular patterns (PAMPs) and damage-associated molecular patterns (DAMPs) with Pattern Recognition Receptors (PRRs) (Wiersinga et al. 2014). PAMPs are related to septic microorganisms that include peptidoglycan, lipoplysaccharide (LPS), flagella and lipoteichoic acid (Yoshimura et al. 1999; Hayashi et al. 2001; Akira et al. 2006) while DAMPs are endogenous products released from cells upon cellular injury (Willart and Lambrecht 2009) with heat shock proteins (HSPs), high mobility group box-1 (HMGB1), fibrinogen and hyaluran related to sepsis pathology (Cinel and Opal 2009). Innate immune cells such as macrophages, leukocytes and dendritic cells possess PRRs on their exterior surface (Janeway and Medzhitov 2002). Toll like receptors (TLRs) are PRRs with TLR4 specifically playing an important role in the inflammatory stage of sepsis (Wiersinga 2011). When TLR4 interacts with the various PAMPs and DAMPs, multiple transcriptional factors are activated, most importantly the nuclear factor, NF-κβ, that further activates genes causing elevated blood levels of pro-inflammatory cytokines (Janeway et al. 2001; O'Neill et al. 2007; Castellheim et al. 2009). Moreover, after being triggered by an overwhelming initial stimulus, neutrophils and macrophages activate the complement system (Janeway et al. 2001). The clotting cascade pathway is enhanced by cell adhesion of the neutrophil–endothelial system and leukocyte-endothelial system resulting in endothelial cell impairment (Granger and Senchenkova 2010). Nitric Oxide (NO), which is a potent vasodilator, is elevated in the inflammatory phase of sepsis along with reactive oxygen species (ROS) also present in very high amounts compared to the antioxidant levels (Galley 2011).

Renal Structure

       The kidney's role in the human body is exceptional in that it helps to maintain the overall

homeostasis by controlling water and electrolyte levels, acid/base balance, blood pressure and

waste products excretion (Koeppen 2009; Wadei et al. 2012). The kidneys receive around 10-

25% of the cardiac output, which is supplied by the renal arteries (Young 2010; Basile et al.

2012). The blood then undergoes several processes through the afferent arteriole including

glomerular filtration, tubular reabsorption and secretion. These three steps lead to urine

formation that is excreted and constitutes only 1% of the primary filtered blood. There are

around one million nephrons in the kidney, each consisting of the renal corpuscles and different

types of tubules (Murawski et al. 2010). The two main structures in the kidney are the cortex and

the medulla. The cortex receives the greater blood supply (Badzynska et al. 2002) with renal

corpuscles and distal and proximal convoluted tubules present in that region. The medulla has

Loops of Henle and the collecting ducts. Glomerular filtration is the primary process that affects

the body's fluid where urine formation begins (Holecheck 2003). This occurs in the renal

corpuscles that are made up of the glomerulus and the Bowman's capsule (Pollak et al. 2014).

The urinary/Bowman's space is the space between the Bowman's capsule and the glomerulus

and this is where the glomerular plasma filtrate collects as it leaves the capillaries through

the filtration membrane (Pollak et al. 2014). The filtrate is further modified as it passes through

the nephron by tubular reabsorption and/or tubular secretion (Blaine et al. 2015). After leaving

the Bowman's space, the filtrate passes through the proximal convoluted tubules by reabsorbing

certain amounts of the salt, water and electrolytes (Blaine et al. 2015). Then it further passes

through the descending and ascending Loops of Henle, the distal convoluted tubule and finally

the collecting duct. Tubular and glomerular injury may occur due to alterations in structure of

endothelial cells where neutrophils, macrophages, natural killer cells and lymphocytes pass in large amounts into the kidneys (Kinsey and Okusa 2012). This may lead to a dysfunction in the reabsorption and secretory mechanisms as well as the glomerular permeability. Visible damage to renal structures may vary, according to severity, from small changes in cellular morphology to tubular necrosis, also known as acute tubular necrosis (ATN) (Basile et al. 2012).

Glomerular filtration rate (GFR) may be determined from the equation of Net Filtration Pressure (NFP) where $NFP = P_c - P_B - \pi_c$ (P_c is the hydrostatic pressure in the glomerular capillaries, P_B is the hydrostatic pressure in Bowman's space and π_c is the oncotic pressure in the glomerular capillaries; Kellum 2015). The hydrostatic pressure is the pressure exerted directly by fluid on the capillary walls of the glomerulus or Bowman's capsule (Deshmukh et al. 2009).

Researchers found that cystatin C (CystC) in the blood is not influenced by sepsis and therefore is a potentially valuable specific and sensitive marker of kidney function in septic conditions (Gerbes et al 2002; Schuck et al. 2002; Mårtensson et al. 2012). CystC is a cysteine protease inhibitor found in the lysosomes of all nucleated cells and participates in protein metabolism inside the cell (Abrahamson et al 1990; Laterza et al. 2002). In the kidney, CystC is filtered in the glomerulus, reabsorbed, degraded by the proximal tubules' epithelium and passed into the urine (Tenstad et al. 1996; Zappitelli et al. 2006). Neither inflammation, weight, muscle mass, gender nor diet may affect the CystC value (Grubb et al. 1985; Simonsen et al. 1985; Abrahamson et al 1990). Moreover, CystC may be useful for determining GFR (Finney et al. 2000) since in several studies, an obvious relationship was linked between the CystC and GFR in adults (Simonsen et al. 1985; Bökenkamp et al. 1998)

Sepsis and Acute Kidney Injury

As sepsis severity increases in patients, the risk factor of development of acute kidney injury (AKI) also increases (Lopes et al. 2009). It was found that 26% to 50% of patients who developed AKI had sepsis already present initially, compared with only 7% to 10% who had primary kidney disease–associated AKI (Bagshaw et al. 2008). AKI leads to an impaired generation of urine, hypertension by reabsorbing excess water and salt and an imbalance between acid/base and electrolyte homeostasis (Morrell et al. 2014; Blaine et al. 2015).

Sepsis-associated AKI (SA-AKI) carries a different pathophysiology and a higher severity of illness than AKI not related to sepsis, and therefore different therapeutic interventions should be given (Alobaidi et al. 2015). Although SA-AKI incidence is 50% (Alobaidi et al. 2015), its pathophysiology is not completely known yet with no specific therapy present (Doyle and Forni 2016). Recent studies have suggested that SA-AKI might not be always linked with a decrease in renal blood flow (RBF) due to a decrease in cardiac output (Alobaidi et al. 2015). In fact, even if the RBF is not decreased, distortion in the renal microcirculation may still happen (Legrand and Payen 2011). In addition, low blood pressure was not correlated with AKI in critically ill patients with severe sepsis (Chawla et al. 2007). An important hemodynamic concept proposed in SA-AKI is elevated renal vascular resistance (RVR) with microvascular distortions in the kidney leading to intraglomerular thrombosis (Zarbock et al. 2014). Unfortunately, treatment of SA-AKI has advanced little during the last several decades and therefore, more studies are needed to investigate the renal microvascular alterations that occur during SA-AKI.

The Sympathetic Nervous System

Recent studies have proposed that the autonomic nervous system (ANS) may have an influence on the inflammatory response, therefore sepsis might not only affect the immune system but might also interact with the ANS (Tracey 2002; Flierl 2007). The sympathetic nervous system (SNS) in the kidney is vital for blood pressure regulation, water and electrolyte reabsorption and renin secretion (Ritz et al. 1998). Catecholamines such as NE, EPI and dopamine (DA) play an important role after being released in the circulation during the flight/fight response when the SNS is stimulated (McCorry 2007). In the initial stages of sepsis, elevated concentrations of catecholamines such as EPI and NE are present in the circulation that enhances the initial inflammatory response (Rittirsch et al. 2008). Previously, it was believed that catecholamine synthesis was related solely to the SNS; however leukocytes and phagocytes may also contribute to the catecholamine synthesis as leukocytes also express adrenergic receptors (Bergquist et al. 1994; Flierl 2007).

During sepsis, the catecholamines are increased in the circulation and when they interact with the adrenergic receptors in the kidneys, this may cause a vasoconstriction of afferent arterioles that may lead to a decrease in RBF (Casellas et al. 1985). NE is the main neurotransmitter released by the renal sympathetic nerves (Pongratz and Straub 2014) with its effects exerted on the kidney passing through β1-adrenergic receptors in juxtaglomerular cells that elevate renin secretion and helps regulate blood pressure (Kopp 2011). Studies have shown that nerve endings of glomerular arterioles and juxtaglomerulus apparatus (JGA) in the kidney have NE and therefore are sympathetic nerves (Barajas 1979).

When there is an elevated level of renal SNS activity and an activation of efferent sympathetic nerves, α1 and β1 adrenergic receptors are stimulated that lead to renin release, a decrease in RBF along with increased reabsorption of sodium and fluid retention (Wyss and Carlson 1999). The renin-angiotensin system is also activated through the feedback mechanism with the ANS and therefore leads to an exacerbated level of SNS activity (Manrique et al. 2009). This elevated level of SNS activation may constitute deleterious effects on the kidney due to the prolonged vasoconstriction on afferent arterioles that consequently leads to a decrease in RBF (Smyth et al. 1985; Kannan et al. 2014). In conclusion, the adrenergic receptors stimulated due to SNS activation during initial stages of sepsis stimulates the pro-inflammatory responses and worsens the adverse effects, although the complete pathways that cause these effects are still to be investigated.

Hypothesis and Specific Aims

The level of sympathetic nerve activation is a major determinant of RBF and GFR. Sepsis, like other stress conditions, is characterized by an increase in the sympathetic nerve activity (SNA), as shown by the increase in plasma catecholamine levels, and in directly recorded SNA (Hahn et al. 1995). There is evidence that sepsis can induce sprouting in sympathetic nerve fibers as studies have shown elevated tyrosine hydroxylase (TH) expression in the gut of septic rats at both 2 h and 20 h where sepsis was induced by CLP (Zhou et al. 2004). TH is the rate limiting enzyme in the catecholamine synthesis pathway. Moreover, rheumatoid arthritis (RA) elevated the sympathetic nerve fiber density in the spleen of a rat model (Lorton et al. 2005). In another study, sympathetic nervous activity was elevated in the heart and kidney of conscious septic sheep model induced by intravenous administration of *E. coli*. In the kidney, the effect was only seen after 20 h (Calzavacca et al. 2014).

A previous study has shown that sympathetic nerve fiber density in the spleen was elevated during acute sepsis due to a neuronal sprouting response (Hoover et al. 2014). The researchers used the same sepsis model in our experiments, and there was an upregulation of nerve growth factor (NGF) in the spleen and consequent rapid growth of noradrenergic nerve fibers. This finding suggests the possibility that the effects of NGF could be widespread in sepsis. Therefore, to test if the same effect is happening in the kidney we conducted this project. Our hypothesis was that during sepsis, which is a stressful situation, the renal sympathetic innervation will increase. Furthermore, we proposed that the renal sympathetic innervation will increase 16 h after CLP, and so if prolonged, it may lead to vasoconstriction of afferent arterioles in the kidney that might be detrimental to kidney function in hindering the normal filtration process from occurring with renal structural changes evident.

The first aim was to evaluate the renal sympathetic nerve abundance and renal non-neuronal cholinergic cells during sepsis using ChAT-eGFP mice. ChAT-eGFP mice have the GFP (green fluorescent protein) gene inserted downstream of the promoter for choline acetyltransferase (ChAT), the enzyme required for the synthesis of acetylcholine. The first aim was achieved by:

1. Immunolabelling the kidney tissues for the sympathetic nerve marker, TH and for GFP to identify non-neuronal cholinergic cells.

2. Analyzing confocal microscopic images for TH nerves and GFP non-neuronal cholinergic cells.

3. Measuring TH and GFP protein content in our kidney samples by western blotting

4. Measuring renal catecholamines by high performance liquid chromatography (HPLC).

The second aim was to investigate the renal morphological and functional changes by:

5. Staining the kidney tissues with Hematoxylin and eosin (H & E) and periodic acid schiff (PAS) reagents.

6. Measuring the renal function using serum CystC as the marker

CHAPTER 2

MATERIALS AND METHODS

Animals Used

Wild-type C57BL/6 adult male mice were purchased from Harlan Laboratories and

used to investigate renal morphology, histology, and CystC levels. Male ChAT-eGFP

transgenic mice were purchased from Jackson Laboratories and used for western blotting,

renal catecholamine measurements, and immunohistochemistry. Both strains of mice used

in the experiments were 4-6 months of age.

The animals had a light/dark cycle of 12 hours each with access to food and water in

their respective cages. Animal protocols were approved by the East Tennessee State

University Committee on Animal Care and conformed to guidelines of the National

Institutes of Health as published in the *Guide for the Care and Use of Laboratory*

Animals (Eight Edition, National Academy of Sciences, 2011). All mice were maintained

in the Division of Laboratory Animal Resources at ETSU.

Cecal Ligation and Puncture (CLP) Surgery

CLP was the surgical method used to induce polymicrobial sepsis in male C57BL/6 and

ChAT-eGFP mice. Both strains were 4-6 months of age at the time of surgery. Anesthesia was

induced with 5% isoflurane (100% O_2 at 1 ml/min) in a separate chamber. Mice were transferred

to the surgery area, and 2% isoflurane was used to maintain anesthesia during the surgery

procedure. The cecum was externalized through a 1 cm abdominal midline incision. The entire

cecum was then ligated just distal to the ileocecal junction with a 0 suture and punctured once

with a 20 gauge needle in an avascular region near the distal end. After manually extruding a

small amount of feces from the puncture site, the cecum was reinternalized and the abdomen was closed in two layers. The mice then received a subcutaneous injection of resuscitation fluid (1 mL lactated Ringers solution) after surgery. The mice never received a post-surgery antibiotic. Mice were euthanized with isoflurane anesthetic 16 h post-surgery. Sham mice were used as a control for surgery, as they underwent similar surgery to the CLP procedure, but without ligation or puncture of cecum. Instead the cecum was externalized and then immediately reinternalized.

Immunohistochemistry

ChAT-eGFP mice were already available, and we decided to use them for investigating our main aim which was looking at the renal sympathetic nerve density 16 h after sepsis surgery. Use of these transgenic mice allowed us to also investigate the presence of non-neuronal cholinergic cells (i.e., eGFP+) in the kidney and determine if the abundance of these cells was altered in sepsis. Therefore, the kidney tissues were double-labeled for the sympathetic nerve marker TH, a rate limiting enzyme for biosynthesis of catecholamines, and for eGFP.

ChAT-eGFP mice that underwent CLP and sham surgeries were euthanized with isoflurane at 16 h post-surgery. Kidneys were collected and stored in 4% paraformaldehyde in 0.01M PBS at 4°C overnight. They were then cryoprotected in 20% sucrose, frozen in dry ice and stored at -80°C. Frozen, 100 μm longitudinal kidney sections of CLP and sham mice were cut using a cryostat and stained free-floating in a 12-well culture plate. After the kidney tissue was cut, the renal sections were rinsed four times in 0.1M PBS, 10 minutes each. Then they were incubated with permeabilizing solution (0.5% BSA + 0.4% Triton X-100) in PBS for 20 min at room temperature. Tissues were then incubated in blocking solution (10% Normal Donkey Serum in 1% BSA + 0.4% Triton-X100 in PBS) for 2 h at room temperature. Kidney sections

were incubated for two days at 4°C following the application of the primary antibodies, anti-tyrosine hydroxylase rabbit polyclonal antibody (1:500 dilution, Pel-Freez, P40101-150) and anti-GFP chicken polyclonal antibody (1:2000 dilution, Abcam AB13970) in 1% BSA + 0.4% Triton X-100 in PBS. After two days, the tissues were washed with 0.1M PBS five times, 10 min each and rinsed with permeabilizing solution (0.5% BSA + 0.4% Triton X-100) in PBS for 20 min at room temperature. Tissues were then stained with AlexaFluor® 594 conjugated donkey anti-rabbit (1:200, Molecular Probes, A21207) and AlexaFluor® 488 conjugated donkey anti-chicken (1:200, Jackson ImmunoResearch, 703545155). The secondary antibodies were left on overnight at 4°C. Tissues were then washed with 0.1M PBS six times and placed on slides. Coverglasses were attached using CitiFluor mounting medium.

Confocal Microscopy

The kidney tissues obtained from immunohistochemistry were visualized under a confocal laser-scanning microscope. Confocal images were obtained with a Leica TCS SP8 Confocal Microscope system with dual line switching excitation (488 nm and 543 nm). Confocal microscopy was used to capture images of the double-labeled kidney tissues. 90 optical sections were collected per field, and multiple fields were stitched together to create a montage. Maximum projection images of three montages were evaluated per mouse. TH nerve density and GFP cell density of each CLP and sham confocal image was quantified using ImageJ software, and group values were compared using a two way-unpaired t-test.

Renal Morphology and Histology

The next aim was to investigate if acute sepsis resulted in any renal pathological changes. C57BL/6 mice were euthanized 16 h after surgery and the left kidneys were collected and fixed in formalin overnight. The next day, the kidneys were put in 70% ethanol and embedded in paraffin. Using a microtome (Microm), 5 μm short axis sections were cut. Routine Hematoxylin and Eosin (H & E) staining as well as Periodic acid–Schiff (PAS) Staining were done to look at renal morphology. Images of the renal corpuscles were collected at 40X magnification using a microscope equipped with a digital camera and QCapture software. Stereo Investigator software was used to measure the area of the glomerulus and Bowman's capsule of each renal corpuscle. In addition, the area of the Bowman's space in each renal corpuscle measured was calculated by subtracting the area of the glomerulus from the area of the Bowman's capsule. 90 total renal corpuscles were analyzed, 15 from each mouse (n=3 per group). Measurements were analyzed by an unpaired t-test.

Western Blot of TH and GFP

To analyze TH and GFP protein content in the kidneys, western blot analysis was done. Kidney tissue samples were dissected, frozen in liquid nitrogen, and stored at $-80°C$. Later on, kidneys were thawed and weighed. Thawed kidneys had 100X times buffer added according to their individual weights. The buffer consisted of ice-cold 10X PBS and 1% Tween 20 with Halt protease and phosphatase inhibitor cocktail (Thermo Scientific, 78440). Each kidney was homogenized with a hand-held homogenizer for 10 s per sample and placed back on ice. Then the homogenized samples were centrifuged at 10,000 rpm for 20 min in Eppendorf tubes. The supernatant was then removed and aliquoted into 100 μl tubes for storage at $-20°C$. The protein

concentration of tissue lysates was determined by a BCA Protein Assay Kit (Thermo Scientific, T23227). After the calculated protein and Lamellil Buffer (NuPage LDS Sample Buffer 4X, Thermo Scientific, NP0008) were added, the samples were vortex-mixed for 5 s, boiled for 5 min and then centrifuged for 5 s. 20 µg protein/sample aliquots with a total volume of 20 µL/well were separated on 4-12% Bis-Tris Gel (NuPage Novex, NP0335BOX) for 50 min at 200V with MOPS SDS Running Buffer (NuPage, NP0001). Proteins from the gel were then electrophoretically transferred onto a 0.45-µm nitrocellulose membrane (Amersham Protran, 10600002) using Tris-Glycine Transfer Buffer (Fisher BioReagents, BP1306-4). Blots were washed in PBS and Tween 20. The membrane was blocked in a 2.5% BSA buffer and the membranes were incubated at 4°C overnight with the respective antibodies in 0.1M PBS: anti-tyrosine hydroxylase rabbit polyclonal antibody (1:2000 dilution, Pel-Freez, P40101-150) , anti-GFP chicken polyclonal antibody (1:4000 dilution, Abcam, AB13970) and anti-β actin rabbit polyclonal antibody (1:500 dilution, Thermo Scientific, RB9421P0) to normalize for protein loading. The following day, the membrane was washed twice with PBS and Tween 20 before being incubated with a goat anti-chicken horseradish peroxidase (HRP)-linked antibody (1:5000 dilution, Jackson-ImmunoResearch, 103-035-155) and goat anti-rabbit HRP conjugate (1:5000 dilution, Jackson- ImmunoResearch) for 2 h at room temperature and then washed three times. The proteins on the membrane blots were developed by exposing them to Super Signal West Dura Extended Duration Substrate (Thermo Scientific, 34075) by using 2 ml of each of bottles A and B. Images were generated using G:BOX (Syngene) and the intensity of the luminescent signal of the resulting bands was captured by Quantity One Software (Bio-Rad Laboratories). In the volume analysis settings of the software, local background subtraction method was selected with the data units to be intensity. For each of the CLP and sham kidney samples, TH was

normalized by dividing the adjusted volume of TH by the respective β-actin adjusted volume for each sample. Similarly for GFP, the adjusted volumes of GFP was divided by the respective adjusted volume of β-actin. The normalized data measurements were analyzed between the sham and CLP groups using an unpaired t-test.

Measurement of Renal Catecholamines

C57BL/6 mice were euthanized 16 h after surgery and perfused with 0.1M PBS for around 3 min through the left ventricle to remove plasma catecholamines. The right kidneys were then dissected, flash frozen in liquid nitrogen and finally stored at -80°C. Kidneys were separately weighed and inserted in a 2ml microcentrifuge tube with a ceramic bead where 1ml of buffer (0.1M perchlorate with 1μg/ml dihydroxybenzoic acid (DHBA) as internal standard) was added to each kidney sample tube. Using a FastPrep-24 tissue homogenizer (MP Biomedicals, 116004500), the kidneys were homogenized at 4.0 M/S for 10 sec three consecutive times. While in the same tube, they were centrifuged at 13,000 rpm for 10 min. 700 μl of supernatant was transferred to a CoStar-Spin-X centrifuge filter tube (0.22 μm, prewashed with 700 μl 0.1M perchlorate) and centrifuged at 13,000 rpm for 6 min. The tube filter was then removed and the samples were vortex-mixed. Finally, 50 μl of each sample filtrate was added to 150 μl of 0.1M perchlorate in a 300 μl TPX HPLC vial with a silicone/PTFE septa screw-cap (MicroSolv™) and refrigerated in a 4°C autosampler tray. The injection volume was 5 μl and each sample was analyzed for a duration of 40 min at a range of 20nA. The HPLC setup consisted of Antec Decade ‖ Analyzer with VT-03 flow cell, ISAAC electrode and ALF-115 column (C18) with the oven temperature set at 35°C. The flow rate was 50 μl/min and pressure was 188 bar. The mobile phase composition consisted of 50 mM phosphoric acid, 50 mM citric acid, 8 mM potassium chloride, 0.1 mM EDTA, 10% methanol as an organic solvent, 500 mg/L of 1-octanesulfonic

acid sodium (OSA) and an adjusted pH of 3.25. The peak heights of each of the catecholamines (NE, EPI and DA) were used for the calculations. Catecholamine levels (NE, EPI and DA) were normalized by dividing the peak heights of each catecholamine by the height of DHBA in its respective sample. Afterwards, each ratio was divided by its respective sample kidney weight to obtain renal catecholamine levels. The data measurements were analyzed between the sham and CLP groups using an unpaired t-test.

<div align="center">Measurement of Serum CystC Concentration</div>

C57BL/6 mice were euthanized 16 h after surgery (n =6 per group). Weights were taken that ensured an equal distribution of weights in each group. Immediately after termination, 500 µl of blood was collected from the abdominal vena cava and 150-200 µl of serum was collected from blood using a serum separator. Serum collected from each mouse sample was put on wet ice during collection and further stored at -80°C. Serum was collected in order to measure levels of the protein CystC, an indicator of renal function, using the cystatin C mouse ELISA kit (Biovendor, RD291009200R). The frozen serum samples were prepared for assay by removing them from the -80°C freezer and allowing them to thaw. Afterwards, each serum sample was vortexed for approximately 5 s to ensure homogeneity. The samples were diluted 500x with Dilution Buffer in two steps: 1) 1:10 dilution of serum to Dilution Buffer, which was prepared by combining 10 µl of serum with 90 µl of Dilution Buffer (Solution A) and 2) 1:500 dilution of solution A to Dilution Buffer, which was prepared by combining 10 µl of Dilution A with 490 µl of Dilution Buffer (Dilution B). All dilutions were vortexed after combining to ensure homogeneity. Standards and controls were prepared according to instructions using Dilution Buffer. 100 µl diluted standards, positive and negative controls, a blank, and samples were pipetted into the appropriate wells of the plate, in duplicate. The plate was incubated at room

temperature for 1 h on a plate shaker at 300 rpm. The wells were then washed three times using a multi-channel pipette with 350 μl of Wash Solution. After aspirating the Wash Solution from each well during the third wash, the plate was inverted and tapped firmly against bench paper to ensure each well was dry. 100 μl of Biotin Labelled Antibody was then added into each well. The previously described steps of incubating, shaking, washing, and inverting the plate were repeated. 100 μl of Streptavidin-HRP Conjugate was added to each well. The plate was incubated for 30 min, as previously described, and then inverted. 100 μl of Substrate Solution was added to each well. Aluminum foil was used to cover the plate and the substrate solution was allowed to incubate for 10 min at room temperature. At 10 min, 100 μl of Stop Solution was added to each well to stop the color development. Finally the absorbance of each well was obtained using a microplate reader set to 450 nm with reference wavelength set to 600 nm. The readings at 600 nm were subtracted from the readings at 450 nm. After subtraction, the mean absorbance was calculated for the duplicate standard absorbance readings. The standard curve was drawn by plotting the mean absorbance of the standards against their known concentrations and fit to symmetrical sigmoidal regression. From the standard curve, the measured concentration of diluted samples were obtained. The actual serum CystC concentrations were calculated by adjusting for the dilution factor (multiplying by 500), to obtain a concentration of ng/ml. Serum CystC concentrations were compared between sham and CLP groups and analyzed using an unpaired t-test.

<u>Statistical Analysis</u>

Graph Pad Prism 6 was used for the statistical analysis and generation of graphs. The groups being compared were CLP and sham in the measurements of the Bowman's space area,

25

serum CystC concentration, TH nerve and eGFP non-neuronal density, TH and eGFP protein

content, and renal catecholamines. Data were summarized by the mean and standard error

(SEM). Group mean responses were compared by two-tailed unpaired t-test where p-values of

0.05 or smaller were considered significant.

CHAPTER 3

RESULTS

CLP Renal Tubules Had Bubble Cells Present

To investigate the renal morphological and structural changes in septic kidneys,

hematoxylin and eosin (H & E) (Figure 1) and periodic acid Schiff (PAS) (Figure 2) staining of

the kidney tissues was done. The H & E staining revealed bubble cells in the cortical renal

tubules of the CLP mice with none present in the sham group. Graber et al. suggested that these

bubble cells represent viable renal tubular cells that have been injured sub-lethally (Graber et al

1991). This acute pathology is thought to be reversible.

CLP   **Sham**
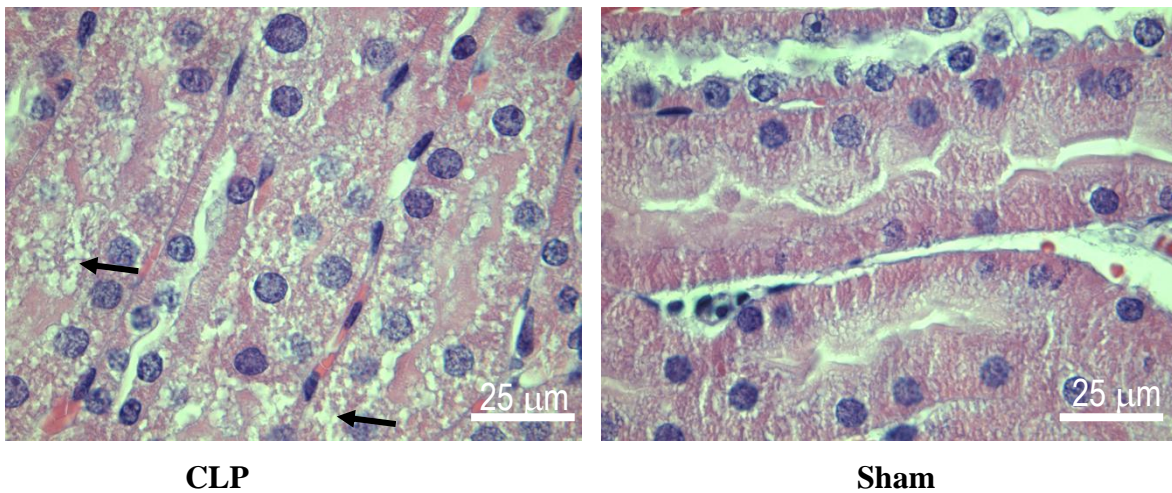
Figure 1: Bubble cells seen in CLP renal tubules 16 h post-surgery. Kidneys of wild type mice
were paraffin-embedded, cut at five microns and stained with H & E. Arrows pointing at bubble
tubular cells. Representative light photomicrographs of each group are shown.

Bowman's Space was Significantly Diminished in Renal Corpuscles of Septic Mice

From the PAS staining photographs (Figure 2), measurements of the area of renal

corpuscle components (i.e., glomerulus, Bowman's capsule and Bowman's space) were done

using Stereo Investigator. Bowman's Space was calculated by subtracting the glomerulus from

the Bowman capsules' area. There was a statistically significant decrease in Bowman's space area in the CLP kidneys compared to the sham kidneys 16 h post surgery. (Sham: 633 ± 92 and CLP: 304 ± 33 µm²; n=3 per group, p = 0.0279). This may indicate a disruption in the glomerular filtration capacity of the CLP kidneys.

A.
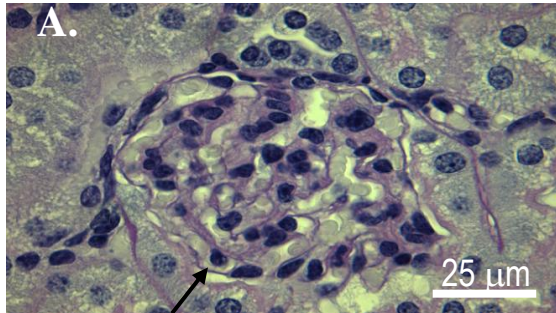
B.
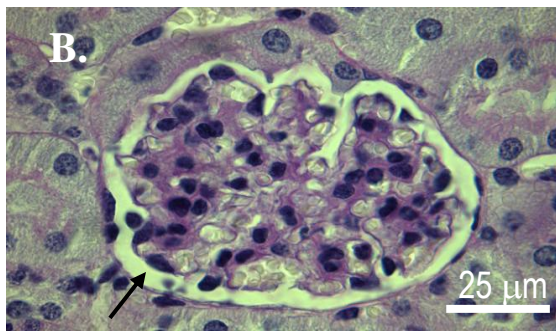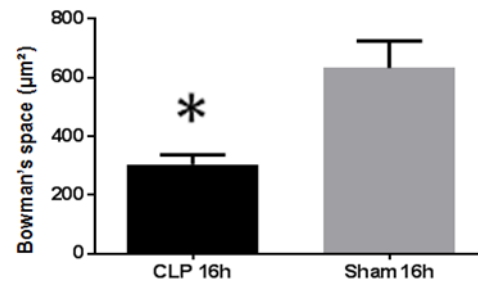
Figure 2: Light photomicrographs of PAS Stained kidneys. **A.** Diminished Bowman's space in (A) CLP renal corpuscles compared to (B) Sham renal corpuscles of wild type mice. Kidneys were paraffin-embedded, cut at five microns, and stained with PAS reagent. Arrows pointing at Bowman's space. **B.** Quantification of Bowman's space of PAS stained kidney tissue. Statistical analysis shows that the CLP mice had significantly smaller Bowman's space than the sham groups (p = 0.0279). Data was expressed as the mean + SEM (n = 3 mice/group).

Renal Function Was Not Impaired in CLP Mice

PAS staining revealed that Bowman's space was diminished in CLP kidneys, and therefore, to further confirm if renal function was reduced, serum CystC was the renal function marker measured. Serum CystC has been indicated to be a more reliable and better marker than serum creatinine for renal function in mice, especially in AKI models (Sahsiver et al. 2009; Song

et al. 2009). Evaluation of the renal function in both groups by ELISA revealed that there was no significant difference in serum CystC levels between sham and CLP groups (Sham: 376 ± 22 and CLP: 325 ± 11 ng/ml; n=6 per group, $p > 0.05$; Figure 3). This indicated that glomerular filtration capacity was not altered although pathological changes were evident.
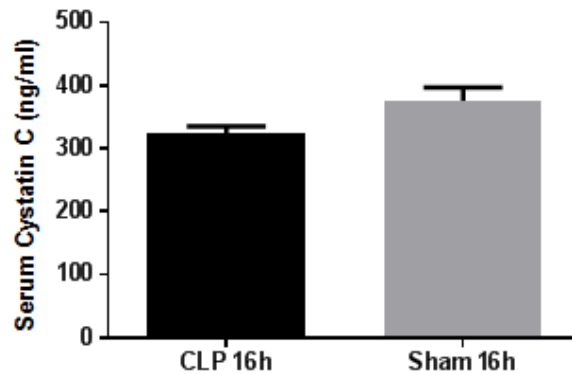
Figure 3. Renal function in septic kidneys 16 h post surgery. Serum was obtained from blood samples by a serum separator and CystC serum levels were measured by cystatin C mouse ELISA kit. No statistical difference in serum CystC levels occurred ($p = 0.0626$). Data was expressed as the mean + SEM (n = 6 mice/group).

Renal Sympathetic Innervation During Sepsis

Since a previous study, using the same model showed that the sympathetic innervation had increased in the spleen (4), our second aim was to evaluate the sympathetic nerve abundance in the kidney during sepsis. Therefore, the kidney tissues were immunolabeled for the sympathetic nerve marker, TH. Confocal microscopic images were obtained and further used for analysis (Figure 4). After analyzing the percentage of TH nerve density present in the renal cortex, there was no significant difference between the two groups. (Sham: 1.43 ± 0.114 and CLP: 2.25 ± 0.297 % area; n=3 per group, $p > 0.05$).
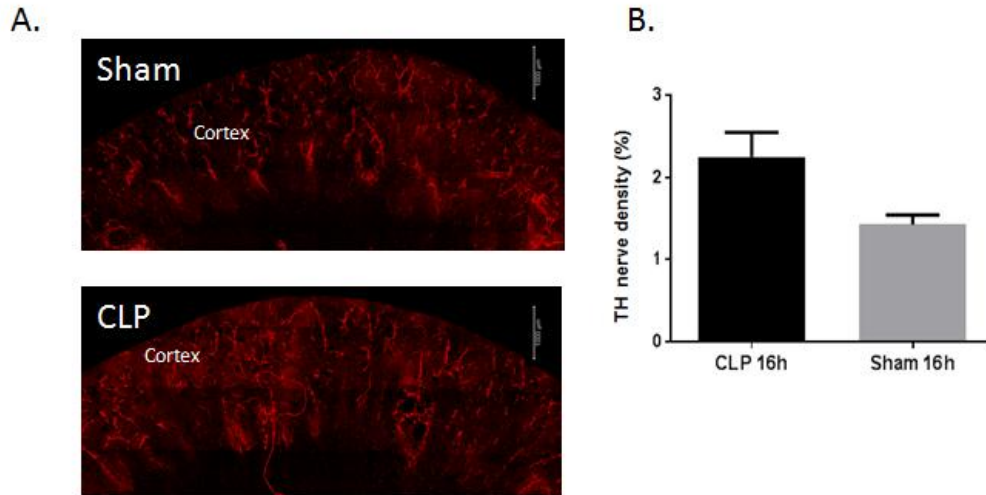
Figure 4: Sympathetic innervation in ChAT-eGFP mice 16 h post-surgery. **A:** Confocal microscopic images of kidney tissue stained with TH post Sham (A) and CLP (B) surgery. Kidney cortical tissue is labeled with AlexaFluor® 594 conjugated donkey anti-rabbit secondary antibody. Bars are 1000 μm. **B:** Quantification of TH nerve density of confocal images using ImageJ. Statistical analysis shows that there was no increase in sympathetic nerve density in septic kidneys ($p = 0.061$). Data was expressed as the mean + SEM (n = 3 mice/group)

Expression of TH in the Kidney

In order to validate the TH nerve density results, we further measured the TH protein content in our kidney samples from both CLP and sham groups by western blotting (Figure 5). In the western blot analysis we studied the whole kidney, while the TH nerve density measurement was focused more on the cortical region of the kidney where the vast majority of nerves are located. Sepsis did not affect the renal TH expression as there was no statistically significant difference between sham and CLP groups. (Sham: 151 ± 22 and CLP: 116 ± 12 (arbitrary units); n=6 per group, $p > 0.05$).
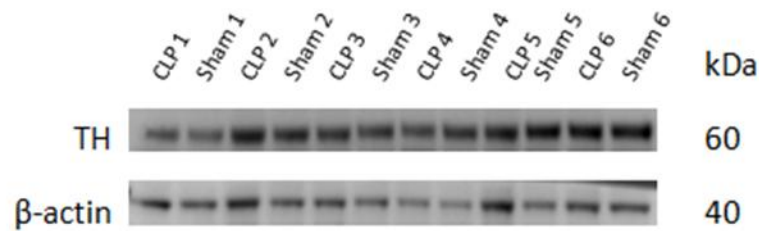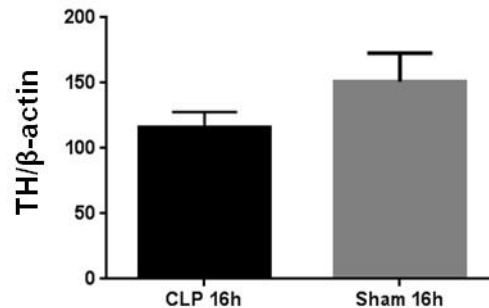
Figure 5: TH protein content in ChAT-eGFP septic kidneys. **A:** Representative Western blot of renal TH protein; **B:** Densitometry of TH bands normalized to β-actin, expressed as arbitrary units with no statistical difference between groups (p = 0.1898). Protein was extracted from the kidney and used for western blot analysis. β-actin was used as loading control. Data was expressed as the mean + SEM (n = 6 mice/group).

As stated previously, TH is the rate limiting enzyme in the catecholamines' synthetic pathway. This pathway includes NE, EPI and DA with NE known to be the main neurotransmitter involved in sympathetic nerves. After measuring renal catecholamines by HPLC at 16 h post-surgery, no differences between groups were detected for NE (Sham: 1331 ± 28 and CLP: 1460 ± 165ng/g), EPI (Sham: 10068 ± 824 and CLP: 11487 ± 1275 ng/g) or DA (Sham: 183 ± 99 and CLP: 162 ± 31 ng/g; n=6 per group, P > 0.05) (Figure 6). This goes hand in hand with our previous TH nerve density results as well as the TH protein expression data that had no change between the two groups.
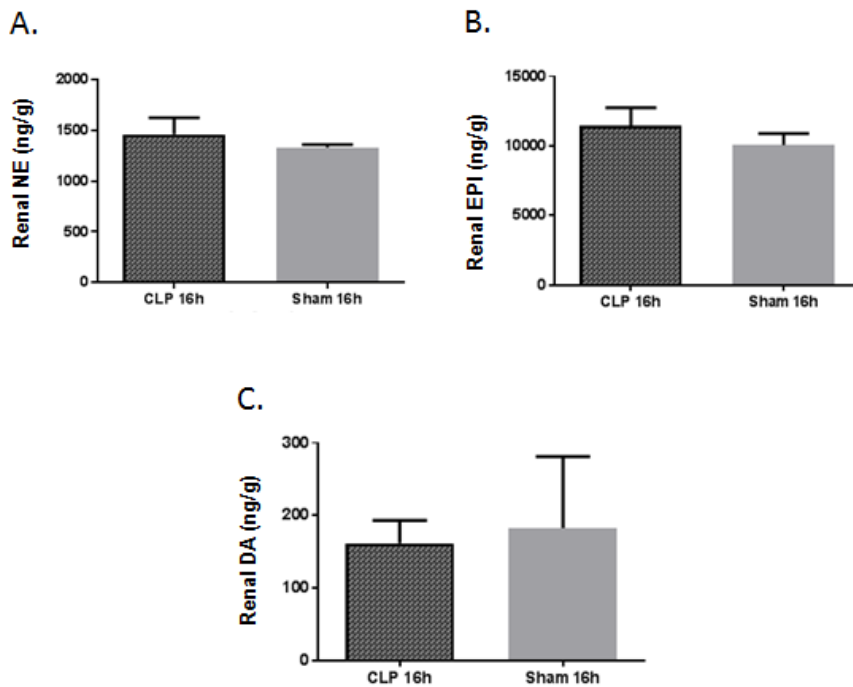
Figure 6. Renal catecholamine levels 16 h post surgery. **A.** NE normalized data. (p = 0.4595) **B.** EPI normalized data. (p = 0.3717) **C.** DA normalized data. (p = 0.8448). Kidneys were homogenized and catecholamine levels were measured by HPLC. DHBA was used as an internal standard. Peak heights of each of the catecholamines were used for analysis. No statistical difference in renal catecholamine levels of ChAT-eGFP mice (p>0.05). Data was expressed as the mean + SEM (n = 6 mice/group).

Non-Neuronal Cholinergic Cells Were Not Altered During Sepsis

The kidney tissues were immunolabeled for eGFP to identify non-neuronal cholinergic cells. Confocal microscopic images were obtained and further used for analysis (Figure 7). After analyzing the percentage of eGFP non-neuronal density present in the renal cortex, there was no significant difference between the two groups. (Sham: 1.43 ± 0.43 and CLP: 0.79 ± 0.05 % area; n=3 per group, $P > 0.05$).
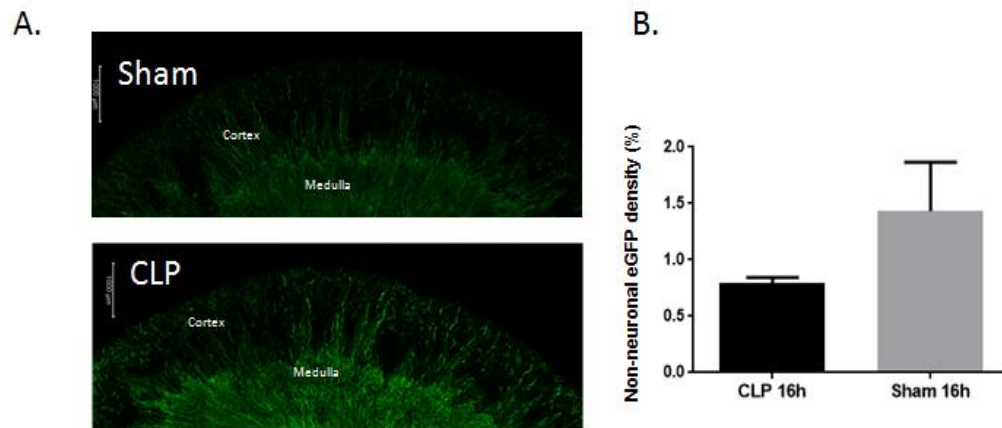
Figure 7: Non-neuronal cholinergic cells during sepsis. **A:** Confocal microscopic images of ChAT-eGFP kidney tissue stained with GFP 16 h post Sham (upper panel) and CLP (lower panel) surgery. Kidney cortical tissue is labeled with AlexaFluor® 488 conjugated donkey anti-chicken secondary antibody. Bars are 1000 μm. **B:** Quantification of GFP non-neuronal density of confocal images using ImageJ. Statistical Analysis shows that there was no significant difference between CLP and sham groups (p = 0.2166). Data was expressed as the mean + SEM (n = 3 mice/group)

Expression of GFP in the Kidney

We then examined the expression of GFP protein in septic and non-septic kidney. As shown by the western blot (Figure 8), there was no statistically significant difference of GFP protein normalized data in kidneys of ChAT-eGFP septic kidneys as compared to kidneys from control mice. (Sham: 101 ± 10 and CLP: 99 ± 8 (arbitrary units); n=6 per group, $P > 0.05$). This reinforced the non-neuronal eGFP density evaluations that also showed no change in the cortical non-neuronal eGFP percentage.

A.
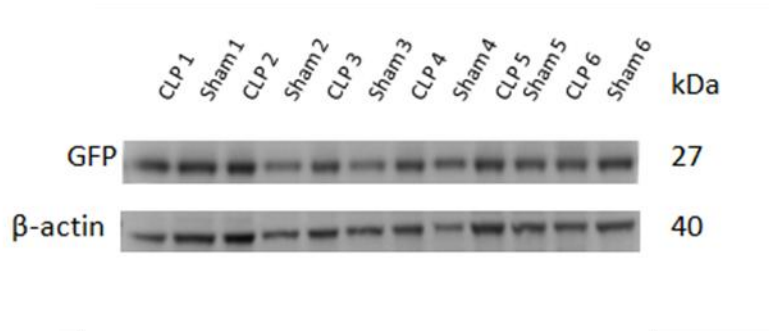
B.
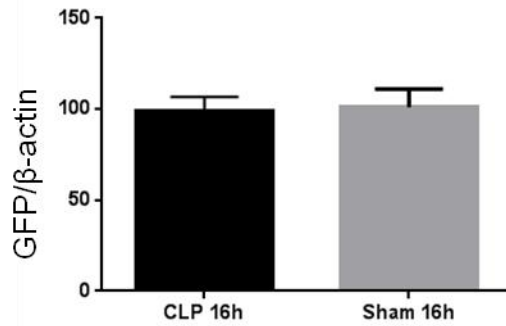
Figure 8. GFP protein content in ChAT-eGFP septic kidneys. A: Representative Western blot of renal GFP protein; B: Densitometry of GFP bands normalized to β-actin, expressed as arbitrary units with no statistical difference between groups (p = 0.8733). Protein was extracted from the kidney and used for western blot analysis of GFP. β-actin was used as loading control. Data was expressed as the mean + SEM (n = 6 mice/group).

CHAPTER 4

DISCUSSION AND CONCLUSIONS

A previous study has shown that sympathetic nerve fiber density in the spleen was elevated during acute sepsis due to a neuronal sprouting response triggered in the spleen (Hoover et al. 2014). The researchers used the same sepsis model as in our experiments, and there was an upregulation of nerve growth factor (NGF) in the spleen and consequent rapid growth of noradrenergic nerve fibers. The researchers proposed that the effects of NGF could be widespread in sepsis. Therefore, to test if the same effect is happening in the kidney we underwent this project. There is evidence that sepsis and rheumatoid arthritis (RA) can induce sprouting in sympathetic nerve fibers as studies have shown elevated TH expression in the gut of septic mice (Zhou et al. 2004), and sympathetic nerve fiber density is increased in the spleen in a RA rat model (Lorton et al. 2005). Our hypothesis was that during sepsis, which is a stressful situation, the renal sympathetic innervation will increase. The present work revealed the effects of acute sepsis on sympathetic innervation of the kidney as well as on renal structural changes and function.

Our findings showed that there was no significant difference in renal sympathetic innervation between the groups during sepsis, after analyzing TH nerve density in the renal cortex (Figure 4). Furthermore, sepsis did not affect the renal TH protein content (Figure 5) as there was no statistically significant difference between the groups. For the TH protein analysis, we studied the whole kidney, while the TH nerve density measurement was focused more on the cortical region of the kidney where the vast majority of nerves are located.

Acute sepsis did not increase the renal sympathetic nerve density by inducing noradrenergic nerve sprouting, which contrasts with the elevated nerve level that occurred in the spleen, although the same septic model was used (Hoover et al. 2014). This difference suggests that sprouting of sympathetic nerves is not a general phenomenon in sepsis and may be limited to lymphoid tissue or related to immune cells solely. Moreover, a prominent difference between both organs is that the spleen is a primary organ for initial response to PAMPs and DAMPs. Furthermore, in the spleen, it was shown that NGF was increased during acute sepsis (Hoover et al. 2014). The mechanism of sympathetic nerve sprouting in the spleen during an inflammatory response is likely that splenocytes produce NGF that binds to neurotrophin receptors on sympathetic neurons, which causes outgrowth of TH-positive neurites into the spleen. In other words, increased NGF synthesis in the spleen during sepsis may have led to an increase in sprouting of sympathetic fibers. In our study, there was no renal sprouting of noradrenergic nerves during sepsis and so this could indicate that increased NGF synthesis and release did not occur.

Since TH is the rate limiting enzyme in the catecholamine synthetic pathway that includes DA, NE and EPI, any change in TH expression should correlate with catecholamine synthesis. After measuring renal catecholamines by HPLC at 16 h post-surgery, no differences between groups were detected for NE, EPI or DA (Figure 6). This goes hand in hand with our previous TH nerve density results as well as the TH protein expression data that had no change between the two groups.

The mice that were used to examine the catecholamine levels were perfused in order for the circulating catecholamines to not affect the measurements. Surprisingly, the mouse kidneys had eight times more epinephrine than norepinephrine in both the sham and CLP

groups. This is most likely due to uptake of circulating epinephrine by renal sympathetic nerves and may have no correlation with the sepsis condition. NE is known to be the main neurotransmitter involved in sympathetic nerves. However, studies have shown that EPI acts on tubular adrenergic receptors and is regulated directly in the kidney by being incorporated into postganglionic sympathetic nerves. EPI is released with NE during renal sympathetic nerve firing for, up to 24 h after its uptake, (Majewski et al. 1981; Quinn et al. 1985; Desir and Peixoto 2013). EPI's main site of action is on β2-receptors with a very high affinity compared to other endogenous compounds (Lands et al. 1967). Renal EPI synthesis may be of importance to renal function as tubular α receptors increase sodium reabsorption and renal β receptors stimulate renin release (Kennedy et al. 1995). N-methylation of NE leads to EPI synthesis, and various N-methylating enzymes are found throughout animals and humans (Kennedy et al. 1995). Of the several enzymes, non-adrenal phenylethanolamine N-methyltransferase (PNMT) is the only one that has been documented to synthesize EPI in vivo (Kennedy et al. 1995). The location of PNMT in the renal glomeruli and tubules suggests that the kidney may synthesize EPI at sites predisposing it to urinary excretion (Kennedy et al. 1995). The rat kidney synthesizes and excretes EPI even with their adrenal glands removed (Ziegler et al. 1989). Similarly, EPI was also found in the urine of humans that had their adrenal glands removed (Von Euler 1961).

Our second part of the study was to examine the effects of acute sepsis on renal structural changes in the kidneys. H & E as well as PAS staining (Figure 1) were done on the kidney tissues. We found that 16 h post-surgery, there were bubble cells visible only in the renal tubules of CLP mice. The bubbles were defined as being clear, homogeneous and spherical in appearance possessing fluid-filled spaces under a light microscope (Racusen et al 1988). Graber

et al. suggested that these bubble cells represent viable renal tubular cells that have been injured sub-lethally (Graber et al 1991). This acute renal pathology is thought to be reversible. The bubble cells were found to be present the highest in patients with ATN and almost always accompanied by normal-appearing renal tubular cells (Graber et al 1991). Moreover, most of the bubble cells excluded trypan blue, indicating normal membrane integrity. Through an electron microscope, no mitochondrial changes were seen in bubble cells that may characterize dead cells. (Graber et al 1991). In addition, LeMasters et al. and Herman et al have defined three stages of cell injury in these models (LeMasters 1987; Herman et al. 1988). In the first and earliest stage of injury, the cells begin to develop clear vesicles while in the second stage the vesicles enlarge and coalesce. Despite the gross distortion of cellular morphology at this time, these stage 2 cells are viable since they exclude trypan blue. Moreover, the vesicles resorb once ischemia is relieved. An irreversible transition from stage 2 to stage 3 happens if there becomes sudden rupture of one of the surface vesicles, after which the cell freely admits trypan blue. A similar vacuolar change is also described in both human ATN and animal models (Taggert et al 1968).

Another important structural change was that Bowman's space was significantly diminished in renal corpuscles of septic mice compared to the sham kidneys 16 h post surgery (Figure 2). This may indicate a disruption in the glomerular filtration capacity in the CLP kidneys. GFR may be determined from the equation of NFP where $NFP = P_c - P_B - \pi_c$. (P_c is the hydrostatic pressure in the glomerular capillaries, P_B is the hydrostatic pressure in Bowman's space and π_c is the oncotic pressure in the glomerular capillaries; Kellum 2015). The hydrostatic pressure is the pressure exerted directly by fluid on the capillary walls of the glomerulus or Bowman's capsule (Deshmukh and Wong 2009). Since the Bowman's space shrinked

significantly in CLP kidneys, this only indicates that there is an increase in hydrostatic pressure in Bowman's space (P_B) which, if the other factors stayed constant, consequently suggests that NFP is decreased and therefore the GFR should decrease as well. However, renal function was not impaired in CLP mice 16 h post-surgery, since there was no significant difference in serum CystC levels (Figure 3). CystC may be useful for determining GFR (Finney et al. 2000) since in several studies, an obvious relationship was linked between the CystC and GFR in adults (Simonsen et al. 1985; Bökenkamp et al. 1998). Moreover, CystC production is not influenced by sepsis and therefore is a potentially valuable specific and sensitive marker of kidney function in septic conditions (Gerbes et al 2002; Schuck et al. 2002; Mårtensson et al. 2012). These results imply that the kidney function is still working properly and that acute sepsis does not cause permanent kidney damage at 16 h in our CLP model although there was a decrease in Bowman's space. Moreover, this may lead us to propose that there are compensatory factors such as the (P_c) and (π_c) that may play a role in allowing normal renal filtration to proceed. However, these factors which are the hydrostatic pressure and oncotic pressure in the glomerular capillaries respectively were undetermined in our experiments. In conclusion, the glomerular filtration capacity or renal function did not seem to be distorted although early, reversible pathological changes were evident in the CLP renal tubules.

The kidneys contain cholinergic tubular cells (GFP+) that are not affected by acute sepsis; however, they may have an important role in renal physiology and pathophysiology. Neither the density of GFP+ cells in confocal analysis nor the abundance of GFP in Western blot was different between the groups after 16hrs in our acute sepsis model (Figure 7 and 8). Several players of the cholinergic system have been found to be present in the renal tubular tissues. This includes acetylcholinesterase enzyme suggesting that acetylcholine (ACh) may be synthesized

from circulating choline in the kidney (Kopp; 2011). In addition, muscarinic ACh receptors (mAChRs) were found in glomeruli, proximal tubules and the collecting duct, so renal ACh may affect solute transport (McArdle et al. 1988; McArdle and Garg 1989; Nitschke et al. 2001; Robey et al. 2001; Johns and Kopp 2012). ChAT has been found in non-neuronal cells that regulates ion and fluid balance (Wessler et al. 2008; Jun et al. 2014). Tubular epithelial cells in the kidney play an important role in the inflammatory response by producing cytokines, growth factors and hormones that affect the function of the non-neuronal cholinergic system, including ACh, through a neural-immune interaction (Wessler and Kirkpatrick 2008). Non-neuronal ACh release is not completely understood; however, during acute inflammatory states, ACh released by the vagal nerve through α7-nAChRs, may have anti-inflammatory effects (Pavlov and Tracey 2005; De Jonge and Ulloa 2007). Moreover, inhibition of the release of proinflammatory mediators such as TNF and IL1-β from immune cells occurs (Pavlov and Tracey 2005; De Jonge and Ulloa 2007).

In conclusion, our hypothesis that there will be an upregulation in sympathetic innervation to the kidney during sepsis was not proven to be true. Neither the TH protein content nor the TH nerve density in the mice kidneys was altered. This differs with the previous spleen model where the noradrenergic nerve sprouting was seen and therefore we may conclude that the sprouting of sympathetic nerves is not a general phenomenon in sepsis and may be limited to lymphoid tissue or related to immune cells solely. Moreover, this may indicate that increased NGF synthesis has not happened. The kidney may not have a bulk of immune cells infiltrating it yet or the kidney may not be in close proximity to the spleen in order for neuro-immune reaction to occur. In addition, acute sepsis did not affect the static measures of the non-neuronal cholinergic system. Bowman's space was diminished with cortical bubble cells present

suggestive of acute renal pathology, however, renal function was unchanged. Furthermore EPI was found to be tremendously higher than NE in our mice kidneys although they were perfused. This may lead us to propose that PNMT found in the kidney may have an important role in regulating EPI synthesis; however, the mechanism and consequences of elevated EPI in mouse kidney are still yet to be determined. Some future aims in working on this project include measuring the NGF in the kidneys during sepsis to see if it is elevated or not. Moreover, using a prolonged septic model (e.g. 24h) may give time for severe renal damage to happen and allow us to investigate if there is a change in sympathetic innervation as well as non-neuronal cholinergic cells expression under these conditions.

REFERENCES

Abrahamson M, Olafsson I, Palsdottir A, Ulvsbäck M, Lundwall A, Jensson O, Grubb A. 1990. Structure and expression of the human cystatin C gene. Biochem. J. 268: 287-294

Akira S, Uematsu S, Takeuchi O. 2006. Pathogen recognition and innate immunity. Cell. 124:783–801.

Alobaidi R, Basu RK, Goldstein SL, Bagshaw SM. 2015. Sepsis-Associated Acute Kidney Injury. Seminars in Nephrology. 35(1): 2–11.

Angus DC, Linde-Zwirble WT, Lidicker J, Clermont G, Carcillo J, Pinsky MR. 2001. Epidemiology of severe sepsis in the United States: analysis of incidence, outcome, and associated costs of care. Crit Care Med. 29:1303–10

Annane D, Bellissant E, Cavaillon JM. 2005. Septic shock. Lancet 365: 63-78.

Badzynska B, Grzelec-Mojzesowicz M, Dobrowolski L, Sadowski J. 2002. Differential effect of angiotensin II on blood circulation in the renal medulla and cortex of anaesthetised rats. J Physiol. 538:159–166.

Bagshaw SM, George C, Bellomo R. 2008. ANZICS Database Management Committee Early acute kidney injury and sepsis: a multicentre evaluation. Crit Care. 12:R47

Barajas L. 1979. Anatomy of the juxtaglomerular apparatus. Am. J. Physiol. 237:F333-F343.

Basile DP, Anderson MD, Sutton TA. 2012. Pathophysiology of Acute Kidney Injury. Comprehensive Physiology. 2(2): 1303–1353.

Beale RJ, Hollenberg SM, Vincent JL, Parrillo JE. 2004. Vasopressor and inotropic support in septic shock: an evidence-based review. Crit Care Med. 32(11 Suppl):S455-65.

Bergmann M, Sautner T. 2002. Immunomodulatory effects of vasoactive catecholamines. Wien Klin Wochenschr. 114:752–761

Bergquist J, Tarkowski A, Ekman R, Ewing A. 1994. Discovery of endogenous catecholamines in lymphocytes and evidence for catecholamine regulation of lymphocyte function via an autocrine loop. Proceedings of the National Academy of Sciences of the United States of America, 91(26): 12912–12916.

Blaine J, Chonchol M, Levi M. 2015. Renal Control of Calcium, Phosphate, and Magnesium Homeostasis. CJASN. 10(7): 1257–1272.

Bökenkamp A, Domanetzki M, Zinck R, Schumann G, Byrd D, Brodehl J. 1998. Cystatin C - a new marker of glomerular filtration rate in children independent of age and height. Pediatrics. 101: 875-881

Boomer JS, Green JM, Hotchkiss RS. 2014. The changing immune system in sepsis: is individualized immuno-modulatory therapy the answer? Virulence. 5:45–56.

Boomer JS, To K, Chang KC, Takasu O, Osborne DF, Walton AH, Bricker TL, Jarman SD, 2nd, Kreisel D, Krupnick AS, Srivastava A, Swanson PE, Green JM, Hotchkiss RS. 2011. Immunosuppression in patients who die of sepsis and multiple organ failure. JAMA. 306(23): 2594–2605

Calzavacca P, May CN, Bellomo R. 2014. Glomerular haemodynamics, the renal sympathetic nervous system and sepsis-induced acute kidney injury. Nephrology, Dialysis, Transplantation.

Casellas D, Carmines PK, Navar LG. 1985. Microvascular reactivity of in vitro blood perfused juxtamedullary nephrons from rats. Kidney Int. 28:752–759

Castellheim A, Brekke OL, Espevik T, Harboe M, Mollnes TE. 2009. Innate immune responses to danger signals in systemic inflammatory response syndrome and sepsis. Scand J Immunol. 69: 479–491

Charalambos AG, Eugenia D, Harry PB, Athanassios S. 2000. Pro- versus Anti-inflammatory Cytokine Profile in Patients with Severe Sepsis: A Marker for Prognosis and Future Therapeutic Options. J Infect Dis. 181(1): 176-180

Chaudhry H, Zhou J, Zhong Y, Ali MM, McGuire F, Nagarkatti PS. 2013. Role of cytokines as a double-edged sword in sepsis. In Vivo. 27: 669–84.

Chawla LS, Seneff MG, Nelson DR, Williams M, Levy H, Kimmel PL. 2007. Elevated plasma concentrations of IL-6 and elevated APACHE II score predict acute kidney injury in patients with severe sepsis. Clin J Am Soc Nephrol. 2: 22–30.

Cinel I, Opal SM. 2009. Molecular biology of inflammation and sepsis: a primer. Crit Care Med. 37:291–304.

Cunha BA, Shea KW. 1996. Fever in the intensive care unit. Infect Dis Clin North Am. Mar 10(1): 185-209

De Jonge WJ, Ulloa L. 2007. The alpha7 nicotinic acetylcholine receptor as a pharmacological target for inflammation. Br J Pharmacol. 151:915–929

Deshmukh SR, Wong NW. 2009. The Renal System Explained: An Illustrated Core Text

Desir GV, Peixoto AJ. 2013. Renalase in hypertension and kidney disease. Nephrol Dial Transplant.

Doyle JF, Forni LG. 2016. Update on sepsis-associated acute kidney injury: emerging targeted therapies. Biologics : Targets & Therapy. 10: 149–156.

Finney H, Newman DJ, Thakkar H, Fell JM, Price CP. 2000. Reference ranges for plasma cystatin C and creatinine measurements in premature infants, neonates, and older children. Arch. Dis. Child. 82: 71-75

Flierl MA. 2007. Phagocyte-derived catecholamines enhance acute inflammatory injury. Nature. 449: 721-725

Gaieski DF, Mikkelsen ME, Band RA. 2010. Impact of time to antibiotics on survival in patients with severe sepsis or septic shock in whom early goal-directed therapy was initiated in the emergency department. Crit Care Med. 38(4):1045–1053

Galley HF. 2011. Oxidative stress and mitochondrial dysfunction in sepsis. Br J Anaesth. 107 (1): 57-64.

Gentile LF, Cuenca AG, Efron PA, Ang D, Bihorac A, McKinley BA, Moldawer LL, Moore FA. 2012. Persistent inflammation and immunosuppression: a common syndrome and new horizon for surgical intensive care. J Trauma Acute Care Surg. 72: 1491–1501.

Gerbes AL, Gulberg V, Bilzer M, Vogeser M. 2002. Evaluation of serum cystatin C concentration as a marker of renal function in patients with cirrhosis of the liver. Gut. 50: 106–110

Giebisch G. 1998. Renal potassium transport: Mechanisms and regulation. Am J Physiol. 274:F817–F833

Graber M, Lane B, Lamia R, and Pastoriza-Munoz E. 1991. Bubble cells: renal tubular cells in the urinary sediment with characteristics of viability. J Am Soc Nephrol 1: 999–1004.

Granger DN, Senchenkova E. 2010. Inflammation and the Microcirculation. San Rafael (CA): Morgan & Claypool Life Sciences. Leukocyte–Endothelial Cell Adhesion. Available from: https://www.ncbi.nlm.nih.gov/books/NBK53380/

Grubb A, Simonsen O, Sturfelt G, Truedsson L, Thysell H. 1985. Serum concentration of cystatin C, factor D and beta 2-microglobulin as a measure of glomerular filtration rate. Acta Med. Scand. 218: 499-503

Grubb A. 1992. Diagnostic value of analysis of cystatin C and protein HC in biological fluids. Clin. Nephrol. 389(Suppl. 1): S20-S27

Hahn PY, Wang P, Tait SM, Ba Z, Reich SS, Chaudry IH. 1995. Sustained elevation in circulating catecholamine levels during polymicrobial sepsis. Shock. 4(4):269–273.

Hayashi F, Smith KD, Ozinsky A, Hawn TR, Yi EC, Goodlett DR, Eng JK, Akira S, Underhill DM, Aderem A. 2001. The innate immune response to bacterial flagellin is mediated by Toll-like receptor 5. Nature. 410:1099–1103

Herman B, Nieminen A-L, Gores GJ, Lemasters JJ. 1988. Irreversible injury in anoxic hepatocytes precipitated by an abrupt increase in plasma membrane permeability. FASEB J. 2:146-151.

Holechek MJ. 2003.Glomerular filtration: an overview. Nephrol Nurs J. 30:285–290.

Hoover DB, Downs AM, Bond CE, Ozment TR, Williams DL. 2014. Increased nerve growth factor expression and increased sympathetic nerve fiber growth in the spleen during sepsis. Shock Society. Shock. 41(2):98

Howell MD, Davis AM. 2017. Management of sepsis and septic shock. JAMA. 317:847

Iskander KN, Osuchowski MF, Stearns-Kurosawa DJ, Kurosawa S, Stepien D, Valentine C, Remick DG. 2013. Sepsis: multiple abnormalities, heterogeneous responses, and evolving understanding. Physiol Rev. 93:1247–88.

Janeway CA Jr, Medzhitov R. 2002. Innate immune recognition. Annu Rev Immunol. 20:197–216.

Janeway CA Jr, Travers P, Walport M. 2001. Immunobiology: The Immune System in Health and Disease. 5th edition. New York: Garland Science. The complement system and innate immunity. Available from: https://www.ncbi.nlm.nih.gov/books/NBK27100/

Johns JE, Kopp UC. 2012. Neural control of renal function. pp. 451–486. In Seidin and Giebisch's The Kidney, 5th ed. (Alperm, R. J., Caplan, M. J. and Moe, O. W. eds.), Elsevier, Amsterdam.

Jun JG, Maeda S, Kuwahara-Otani S, Tanaka K, Hayakawa T, Seki M. 2014. Expression of adrenergic and cholinergic receptors in murine renal intercalated cells. J Vet Med Sci 76:1493–1500

Kalra OP, Raizada A. 2006. Management issues in urinary tract infections. J Gen Med. 18:16–22

Kannan A, Medina RI, Nagajothi N, Balamuthusamy S. 2014. Renal sympathetic nervous system and the effects of denervation on renal arteries. World Journal of Cardiology, 6(8), 814–823.

Kellum JA. 2015. Nephrology, An Issue of Critical Care Clinics, E-Book

Kennedy B, Bigby TD, Ziegler MG. 1995. Nonadrenal epinephrine-forming enzymes in humans. Characteristics, distribution, regulation, and relationship to epinephrine levels. J Clin Invest. 95:2896–2902

Kinsey GR, Okusa MD. 2012. Role of leukocytes in the pathogenesis of acute kidney injury. Critical Care, 16(2), 214.

Koeppen BM. 2009. The kidney and acid-base regulation. Adv Physiol Educ. 33(4):275–281

Kopp UC. 2011. Neural Control of Renal Function. San Rafael (CA): Morgan & Claypool Life Sciences; Chapter 2, NeuroAnatomy.

Lands AM, Arnold A, McAuliff JP, Luduena FP, Brown TG. 1967. Differentiation of receptor systems activated by sympathomimetic amines. Nature (Lond.). 214:597-598

Laterza OF, Price CP, Scott MG. 2002. Cystatin C: an improved estimator of glomerular filtration rate? Clin. Chem. 48: 699-707

Legrand M, Payen D. 2011. Understanding urine output in critically ill patients. Annals of Intensive Care.1: 13.

Lemasters JJ, DiGuiseppi J. Nieminen A-L. 1987. Blebbing. free calcium and mitochondnial membrane potential preceding cell death in hepatocytes. Nature (Lond). 325:78-81

Levy MM, Fink MP, Marshall JC. 2003. International Sepsis Definitions Conference. Crit Care Med. 31:1250–1256

Lopes JA, Jorge S, Resina C, Santos C, Pereira A, Neves J. 2009. Acute kidney injury in patients with sepsis: a contemporary analysis. Int J Infect Dis. 13:176–81.

Lorton D, Lubahn C, Lindquist CA, Schaller J, Washington C, Bellinger DL. 2005. Changes in the density and distribution of sympathetic nerves in spleens from Lewis rats with adjuvant-induced arthritis suggest that an injury and sprouting response occurs. J Comp Neurol. 489:260–273.

Majewski H, Rand M, Tung LH. 1981. Activation of prejunctional B-adrenoreceptors in rat atria by adrenaline applied exogenously or released as a cotransmittor. Br. J. Pharmacol. 73:669–679

Manrique C, Lastra G, Gardner M, Sowers JR. 2009. The Renin Angiotensin Aldosterone System in Hypertension: Roles of Insulin Resistance and Oxidative Stress. The Medical Clinics of North America. 93(3), 569–582.

Mårtensson J, Martling CR, Oldner A, Bell M. 2012. Impact of sepsis on levels of plasma cystatin C in AKI and non-AKI patients. Nephrol. Dial. Transplant. 27: 576-581

Martin GS, Mannino DM, Eaton S, Moss M. 2003. The epidemiology of sepsis in the United States from 1979 through 2000. N Engl J Med. 348:1546–1554

Martin GS. 2012. Sepsis, severe sepsis and septic shock: changes in incidence, pathogens and outcomes. Expert Rev. Anti Infect. Ther. 10:701–706

McArdle S, Garg LC, Crews FT. 1988. Cholinergic stimulation of phosphoinositide hydrolysis in rabbit kidney. J Pharmacol Exp Ther. 244: 586–591

McArdle S, Garg LC. 1989. Cholinergic stimulation of phosphoinositide hydrolysis in renal medullary collecting duct cells. J Pharmacol Exp Ther. 248: 682–686

McCorry LK. 2007. Physiology of the Autonomic Nervous System. American Journal of
Pharmaceutical Education. 71(4), 78.

Morrell ED, Kellum JA, Hallows KR, Pastor-Soler NM. 2014. Epithelial transport during septic
acute kidney injury. Nephrol Dial Transplant. 29 (7): 1312-1319.

Murawski IJ, Maina RW, Gupta IR. 2010. The relationship between nephron number, kidney
size and body weight in two inbred mouse strains. Organogenesis, 6(3), 189–194.

Nitschke R, Henger A, Ricken S, Muller V, Kottgen M, Bek M, Pavenstadt H.
2001. Acetylcholine increases the free intracellular calcium concentration in podocytes in
intact rat glomeruli via muscarinic M5 receptors. J. Am. Soc. Nephrol. 12: 678–687.

Oberbeck R, Schmitz D, Wilsenack K, Schuler M, Pehle B, Schedlowski M, Exton MS. 2004.
Adrenergic modulation of survival and cellular immune functions during polymicrobial
sepsis. Neuroimmunomodulation. 11:214–223

Oberbeck R. 2006. Catecholamines: physiological immunomodulators during health and
illness. Curr Med Chem. 13:1979–1989

O'Neill LA, Bowie AG. 2007. The family of five: TIR-domain-containing adaptors in Toll-like
receptor signalling. Nat Rev Immunol. 7:353–64

Pavlidis TE. 2003. Cellular changes in association with defense mechanisms in intra-abdominal
sepsis. Minerva Chir. 58(6):777-81.

Pavlov VA, Tracey KJ. 2005. The cholinergic anti-inflammatory pathway. Brain Behav
Immun. 19:493–499

Pollak MR, Quaggin SE, Hoenig MP, Dworkin LD. 2014. The glomerulus: the sphere of
influence. Clin J Am Soc Nephrol. 9:1461–1469

Pongratz G, Straub RH. 2014. The sympathetic nervous response in inflammation. Arthritis
Research & Therapy. 16: 504.

Quinn P, Borkowski KR, Collis MG. 1985. Epinephrine enhances neurogenic vasoconstriction in
the rat perfused kidney. Hypertension. 7: 47–52

Racusen LC, Fivush B, Solez K. 1988. Culture of viable cells from urine of patients with "acute
tubular necro-515" (Abstract). Kidney Int. 33:364.

Rangel-Frausto MS, Pittet D, Costigan M, Hwang T, Davis CS, Wenzel RP. 1995. The natural
history of the systemic inflammatory response syndrome (SIRS): a prospective
study. JAMA. 273(2):117–23

Rittirsch D, Flierl MA, Ward PA. 2008. Harmful molecular mechanisms in sepsis. Nature
Reviews. Immunology, 8(10), 776–787.

Ritz E, Amann K, Fliser D. 1998. The sympathetic nervous system and the kidney: Its importance in renal diseases. Blood Press Suppl. 3: 14–19

Robey RB, Ruiz OS, Baniqued J, Mahmud D, Espiritu DJ, Bernardo AA, Arruda JA. 2001. SFKs, Ras, and the classic MAPK pathway couple muscarinic receptor activation to increased Na-HCO3 cotransport activity in renal epithelial cells. Am. J. Physiol. Renal Physiol. 280: F844–F850

Sahsivar MO, Narin C, Kiyici A, Toy H, Ege E, Sarigul A. 2009. The effect of iloprost on renal dysfunction following renal ischemia reperfusion using cystatin C and beta2-microglobulin monitoring. Shock. 32: 498– 502

Samyn M, Cheesam P, Bevis L, Taylor R, Samaroo B, Buxton-Thomas M. Cystatin C, an easy and reliable marker for assessment of renal dysfunction in children with liver disease and after liver transplantation. Liver Transpl 2005; 11: 344–349.

Schuck O, Gottfriedova A, Maly J, Jabor A, Stollova M, Bruzkova I. 2002. Glomerular filtration rate assessment in individuals after orthotopic liver transplantation based on serum cystatin C levels. Liver Transpl. 8: 594–599

Simonsen O, Grubb A, Thysell H. 1985 The blood serum concentration of cystatin C (gamma-trace) as a measure of the glomerular filtration rate. Scand. J. Clin. Lab. Invest. 45: 97-101

Smyth DD, Umemura S, Pettinger WA. 1985. Renal nerve stimulation causes alpha 1-adrenoceptor-mediated sodium retention but not alpha 2-adrenoceptor antagonism of vasopressin. Circ Res. 57(2):304–311

Song S, Meyer M, Turk TR, Wilde B, Feldkamp T, Assert R, Wu K, Kribben A, Witzke O. 2009. Serum cystatin C in mouse models: A reliable and precise marker for renal function and superior to serum creatinine. Nephrol Dial Transplant. 24: 1157– 1161

Taggert WR, Thibodeau GA, Swanson RN. 1968. Mannitol-induced renal alteration in rabbits. S D J Med. 21:30-34.

Tenstad O, Roald AB, Grubb A, Aukland K. 1996. Renal handling of radiolabelled human cystatin C in the rat. Scand. J. Clin. Lab. Invest. 56: 409-414

Torio CM, Moore BJ. 2013. Healthcare Cost and Utilization Project (HCUP) Statistical Briefs. Rockville (MD): Agency for Healthcare Research and Quality (US); 2006. National inpatient hospital costs: the most expensive conditions by payer, statistical brief #204

Tracey KJ. 2002. The inflammatory reflex. Nature. 420:853–859.

Uchino S, Kellum JA, Bellomo R, Doig GS, Morimatsu H. 2005. Acute renal failure in critically ill patients: a multinational, multicenter study. JAMA 294: 813–818

Von Euler US, Ikkos D, Luft R. 1961. Adrenalin excretion during resting conditions and after insulin in adrenalectomized human subjects. Acta. Endocrinol. 38:441-448.

Wadei HM, Textor SC. 2012. The role of the kidney in regulating arterial blood pressure. Nat Rev Nephrol. 8:602-609.

Wessler I, Kirkpatrick CJ. 2008. Acetylcholine beyond neurons: the non-neuronal cholinergic system in humans. British Journal of Pharmacology. 154(8): 1558–1571.

Wiersinga WJ, Leopold SJ, Cranendonk DR, van der Poll T. 2014. Host innate immune responses to sepsis. Virulence. 5: 36–44.

Wiersinga, W. J. 2011. Current insights in sepsis: from pathogenesis to new treatment targets. Curr. Opin. Crit. Care. 17: 480–486

Willart MA, Lambrecht BN. 2009. The danger within: endogenous danger signals, atopy and asthma. Clin Exp Allergy. 39:12–19

Wyss JM, Carlson SH. 1999. The role of the central nervous system in hypertension. Curr Hypertens Rep. 1:246–253

Xiao Z, Wilson C, Robertson HL, Roberts DJ, Ball CG, Jenne CN, Kirkpatrick AW. 2015. Inflammatory mediators in intra-abdominal sepsis or injury – a scoping review. Critical Care, 19, 373.

Yoshimura AE, Lien RR, Ingalls E, Tuomanen R, Dziarsi. 1999. Cutting edge: recognition of Gram-positive bacterial cell wall components by the innate immune system occurs via Toll-like receptor 2. J. Immunol. 163:1-5.

Young DB. 2010. Control of Cardiac Output. San Rafael (CA): Morgan & Claypool Life Sciences. Chapter 1, Introduction.

Zappitelli M, Parvex P, Joseph L, Paradis G, Grey V, Lau S, Bell L. 2006. Derivation and validation of cystatin C-based prediction equations for GFR in children. Am. J. Kidney Dis. 48: 221-230

Zarbock A, Gomez H, Kellum JA. 2014. Sepsis-induced AKI revisited: pathophysiology, prevention and future therapies. Current Opinion in Critical Care. 20(6): 588–595.

Zarjou A, Agarwal A. 2011. Sepsis and acute kidney injury. J Am Soc Nephrol. 22(6):999-1006.

Zeni F, Freeman B, Natanson C. 1997. Anti-inflammatory therapies to treat sepsis and septic shock: a reassessment. Crit. Care Med. 25, 1095–1100

Zhou M, Hank Simms H, Wang P. 2004. Increased gut-derived norepinephrine release in sepsis: up-regulation of intestinal tyrosine hydroxylase. Biochim Biophys Acta. 1689:212–218.

Ziegler MG, Kennedy B, Elayan H. 1989. Rat renal epinephrine synthesis. J Clin Invest. 84: 1130–1133

APPENDIX

Abbreviations

ATN	Acute tubular necrosis
Ach	Acetylcholine
ChAT	Choline acetyltransferase
CLP	Cecal ligation and puncture
CystC	Cystatin C
DA	Dopamine
DAMPs	Damage-associated molecular patterns
DHBA	Dihydroxybenzoic acid
EPI	Epinephrine
GFP	Green fluorescent protein
GFR	Glomerular filtration rate
H	Hours
H and E	Hematoxylin and eosin
HMGB1	High mobility group box 1
HSP	Heat shock protein
IL	Interleukin
LPS	Lipoplysaccharide
M/S	Meters/second
MIN	Minutes
NE	Norepinephrine
NFP	Net filtration pressure
NO	Nitric oxide

OSA	1-octanesulfonic acid sodium
PAMP	Pathogen associated molecular pattern
PAS	Periodic acid schiff
PBS	Phosphate buffer saline
PRR	Pattern recognition receptor
ROS	Reactive oxygen species
S	Seconds
SIRS	Systemic inflammatory response syndrome
SNA	Sympathetic nerve activity
TH	Tyrosine hydroxylase
TLR	Toll like receptor

VITA

TUQA ALKHATEEB

Education:	East Tennessee State University, Johnson City, Tennessee; Biology, MS, 2017- Concentration: Biomedical Sciences
	University of Sharjah, College of Pharmacy, Sharjah, United Arab Emirates; B. Pharm, 2015
Professional Experience:	
	Graduate Teaching Assistant, Biological Sciences Department, East Tennessee State University, Johnson City, Tennessee; 2015-2017
Presentations and Awards:	
	Presented a poster entitled as "Effects of Sepsis on Renal Structure and Sympathetic Innervation in Mice" (Master's research project) in the American Society of Investigative Pathology (ASIP) 2017 Annual Meeting held in conjunction with Experimental Biology.
	First Place in Poster Presentation, Appalachian Student Research Forum (Biomedical and Health Science group), East Tennessee State University, Johnson City, Tennessee, 2017
	First Place in Poster Presentation, Appalachian Student Research Forum (Biomedical and Health Science group), East Tennessee State University, Johnson City, Tennessee, 2016

Honors Graduate from University of Sharjah, College of

Pharmacy, Sharjah, United Arab Emirates, 2015

Association Memberships:

Graduate Professional Student Association (GPSA) Member at

ETSU, September 2016

American Society of Pharmacology and Experimental

Therapeutics (ASPET), December 2016 – Present